Title

A thrombospondin in the anthozoan Nematostella vectensis is associated with the nervous system and upregulated during regeneration

Journal

Biology Open, 2(2)

ISSN

2046-6390

Authors

Tucker, Richard P
Hess, John F
Gong, Qizhi
et al.

Publication Date

2013-02-15

DOI

10.1242/bio.20123103

Peer reviewed

A thrombospondin in the anthozoan *Nematostella vectensis* is associated with the nervous system and upregulated during regeneration

Richard P. Tucker[1,*], John F. Hess[1], Qizhi Gong[1], Katrina Garvey[1], Bradley Shibata[1] and Josephine C. Adams[2,*]

[1]Department of Cell Biology and Human Anatomy, University of California, Davis, CA 95616, USA
[2]School of Biochemistry, University of Bristol, Bristol BS8 1TD, UK
*Authors for correspondence (rptucker@ucdavis.edu; jo.adams@bristol.ac.uk)

Biology Open 2, 217–226
doi: 10.1242/bio.20123103
Received 17th September 2012
Accepted 12th November 2012

Summary

Thrombospondins are multimeric extracellular matrix glycoproteins that play important roles in development, synaptogenesis and wound healing in mammals. We previously identified four putative thrombospondins in the genome of the starlet sea anemone *Nematostella vectensis*. This study presents the first analysis of these thrombospondins, with the goals of understanding fundamental roles of thrombospondins in the Eumetazoa. Reverse transcriptase PCR showed that each of the *N. vectensis* thrombospondins (Nv85341, Nv22035, Nv168100 and Nv30790) is transcribed. Three of the four thrombospondins include an RGD or KGD motif in their thrombospondin type 3 repeats at sites equivalent to mammalian thrombospondins, suggesting ancient roles as RGD integrin ligands. Phylogenetic analysis based on the C-terminal regions demonstrated a high level of sequence diversity between *N. vectensis* thrombospondins. A full-length cDNA sequence was obtained for Nv168100 (NvTSP168100), which has an unusual domain organization. Immunohistochemistry with an antibody to NvTSP168100 revealed labeling of neuron-like cells in the mesoglea of the retractor muscles and the pharynx. *In situ* hybridization and quantitative PCR showed that NvTSP168100 is upregulated during regeneration. Immunohistochemistry of the area of regeneration identified strong immunostaining of the glycocalyx, the carbohydrate-rich matrix coating the epidermis, and electron microscopy identified changes in glycocalyx organization during regeneration. Thus, *N. vectensis* thrombospondins share structural features with thrombospondins from mammals and may have roles in the nervous system and in matrix reorganization during regeneration.

Key words: Cnidaria, Mesoglea, Extracellular matrix, Glycocalyx, Regeneration, Nervous system

Introduction

Thrombospondins are multidomain, calcium-binding extracellular matrix (ECM) glycoproteins that have been most intensively studied in mammals, where they form a gene family of five members (TSP1–5). Mammalian thrombospondins have important roles in angiogenesis, wound healing, tumor progression, cardiovascular biology, the development and maintenance of connective tissues and synaptogenesis. These functions are mediated by interactions with many binding partners including other ECM components, growth factors, matrix proteases, integrins, proteoglycans and other adhesion and signaling receptors (for reviews see Adams and Lawler, 2012; Risher and Eroglu, 2012). Along with SPARC, thrombospondins are the most ancient modulatory adhesion molecules, with many interactions that relate to ECM assembly and remodeling (Mosher and Adams, 2012). In structure, the thrombospondins of mammals fall into two subgroups, A and B, that differ in domain composition in their N-terminal regions and assemble through the action of coiled-coil domains either as homo-trimers (subgroup A; TSP1 and TSP2) or as homo-pentamers (subgroup B; TSP3, TSP4 and TSP5). Gene conservation and similarities of expression patterns suggest that the TSP1–5 family has related functions in many other craniates (Tucker, 1993; Tucker et al., 1995; Urry et al., 1998; McKenzie et al., 2006; Kasprick et al., 2011).

Although many important ECM components are specific to gnathostomes (jawed vertebrates) (Özbek et al., 2010), it is now appreciated that thrombospondins are conserved through most metazoan phyla. The genomes of the purple sea urchin *Stronglyocentrotus purpuratus* and the sea squirt *Ciona intestinalis* contain thrombospondin genes encoding proteins with subgroup A and B domain architectures as well as a protein belonging to an additional subgroup termed DD due to the presence of a "discoidin-like domain" at the N-terminus (Bentley and Adams, 2010). In contrast, most protostomes and early-diverging metazoan species encode a single thrombospondin with, in general, subgroup B-like domain architecture (Bentley and Adams, 2010). Functional studies of thrombospondins in invertebrates have only been carried out in *Drosophila menalogaster*. *D. melanogaster* thrombospondin is a pentameric protein that undergoes interactions with heparin and PS2 integrin

and is functionally essential for the development of muscle–tendon attachment sites (Adams et al., 2003; Chanana et al., 2007; Subramanian et al., 2007; Gilsohn and Volk, 2010). These studies indicate conservation of ECM-related functions and interactions of thrombospondins within bilaterians, yet to date nothing is known about the thrombospondins of diploblasts or other early-diverging metazoa. In view of the high conservation of thrombospondins across the metazoa, such investigations are important for understanding the fundamental roles of thrombospondins in tissues.

Cnidaria form a sister group to bilaterians and are increasingly recognized as important model organisms for studying the genomic and organismal evolution of animals. In contrast to *D. melanogaster* and *Caenorhabditis elegans*, which have undergone extensive gene losses, sequencing of several Cnidarian genomes has illuminated relationships with vertebrates and the possible complexity of the metazoan ancestor (Putnam et al., 2007; Chapman et al., 2010). Cnidaria are defined by having two epithelial cell layers (i.e. they are diploblastic), a single oral body opening and tentacles, a muscular system and nerve net, and cnidoblasts. The outer epidermis and inner gastrodermis are separated by an ECM layer, the mesoglea, that has features of both connective tissue ECM and basement membranes (e.g. Schmid et al., 1999; Tucker et al., 2011). The anthozoan Cnidarian *Nematostella vectensis* is an ustuarine sea anemone that is emerging as a tractable laboratory model with a simple lifecycle (Hand and Uhlinger, 1992; Darling et al., 2005). As part of an overview of the evolution of metazoan ECM, we previously identified four thrombospondin genes in *N. vectensis* (Bentley and Adams, 2010; Özbek et al., 2010). Here we present the first analysis of these thrombospondins and their phylogenetic relationships. We report that a *Nematostella* thrombospondin with an unusual domain composition is expressed in adult polyps and is sharply upregulated during regeneration. The possible functions of this anthozoan thrombospondin that can be surmised from its distinctive patterns of expression indicate interesting parallels and differences with the thrombospondins of vertebrates.

Results

The four thrombospondins of *Nematostella vectensis*

BLAST searches of the *N. vectensis* genome identified four open reading frames that include regions characteristic of thrombospondins, i.e. EGF-like domains, thrombospondin type 3 repeats and a C-terminal L-lectin-like domain. These thrombospondins were previously referred to by us using the JGI transcript identification number preceded by "Nv" (Bentley and Adams, 2010; Özbek et al., 2010), and we continue to use that nomenclature here. Nv85341 (which corresponds to GenBank XP_1639928) is encoded on genome scaffold 11 and Nv22035 is on scaffold 62 (scaffold numbers refer to the JGI *N. vectensis* genome assembly) (Putnam et al., 2007). Nv168100 (which corresponds to GenBank XP_1631622) and Nv30790 are both encoded on scaffold 99, suggesting that these genes may be the result of a lineage-specific gene duplication. Inspection of the domain organizations of all four predicted proteins indicates that none of the predictions corresponded to a full-length thrombospondin sequence (Fig. 1A). The prediction for Nv30790 was extended at the N-terminal end through an overlapping expressed sequence tag (EST), FC258725. The region encoded by the EST included two cysteine residues in a position typical of the pentamerizing thrombospondins (Fig. 1A) (Bentley and Adams, 2010). We confirmed that all four genes are transcribed in adult *N. vectensis* using reverse transcriptase PCR (RT-PCR) (Fig. 1B).

Nematostella vectensis thrombospondins have RGD motifs

The tripeptide RGD acts as an integrin binding motif in some thrombospondins and many other ECM molecules (Ruoslahti, 1996; Bentley and Adams, 2010). RGD and KGD motifs are found in the thrombospondin type 3 repeats of three of the four predicted *N. vectensis* thrombospondins (asterisks in Fig. 1A); these sequences were confirmed in the sequenced RT-PCR products described above. Alignment with the thrombospondin type 3 repeat sequences of human thrombospondins (Fig. 2) demonstrated that the RGD and KGD motifs found in *N. vectensis* thrombospondins are in phylogenetically conserved locations. For example, RGD motifs are found in the second thrombospondin type 3 repeat of human TSP4 and 5, and an RGD motif is found at the same site in the second thrombospondin type 3 repeat of Nv30790. A KGD motif is found in the sixth thrombospondin type 3 repeat of human TSP1 that aligns with an RGD motif in Nv168100 and a KGD motif in Nv22035. Finally, RGD motifs are found in the seventh thrombospondin type 3 repeats of human TSP1 and TSP2 and these align with an RGD motif in Nv22035. It is interesting to note that the 14 residue RGD-containing sequence DTDGDGRGDACDDD found in the sixth thrombospondin type 3 repeat of Nv168100: 1) is identical to the 14 amino acid (aa) RGD-containing sequence found in the second thrombospondin type 3 repeat of human TSP4, 2) is 93% identical to this same region in human TSP5 (i.e. 13 of the 14 residues are identical), and 3) contains the same string of nearby aspartic acids.

Molecular cloning and analysis of a *Nematostella vectensis* thrombospondin

The predicted Nv168100 appeared to be relatively complete, so it was selected for further analysis. The 1151 aa full-length coding sequence (NvTSP168100; GenBank accession number JX680803) (Fig. 1C) was obtained from overlapping PCR products generated using primers based on predicted open reading frame sequences as well as potential open reading frame sequences 3′ and 5′ to the sequences encoding the predicted protein. Following the signal peptide (aa 1–21), the N-terminal domain (aa 22–227) corresponds to a laminin G-like domain, which is canonical for the majority of thrombospondins (Tan et al., 2006; Bentley and Adams, 2010). The sequence from aa 228 to aa 471 is unique and includes a region from approximately aa 228 to aa 329 that is rich in proline, arginine and threonine residues (designated "PRT region") and a region from aa 330 to aa 471 that includes a short predicted coiled coil. BLAST searches of GenBank with the PRT region identified proline-rich regions of around 50% identity in *C. briggsae* XP_002636096 (Fig. 1D) and multiple other hypothetical proteins of *C. briggsae*, and proline-rich regions of around 29–32% identity in a bacterial zinc metalloproteinase (ZP_04776628) and a bacterial cell wall anchor domain protein (ZP_06282692). The functions of these related polypeptide regions are unknown. The C-terminal region of NvTSP168100 consists of four EGF-like domains, a series of thrombospondin type 3 repeats and an L-type-lectin-like domain and thus

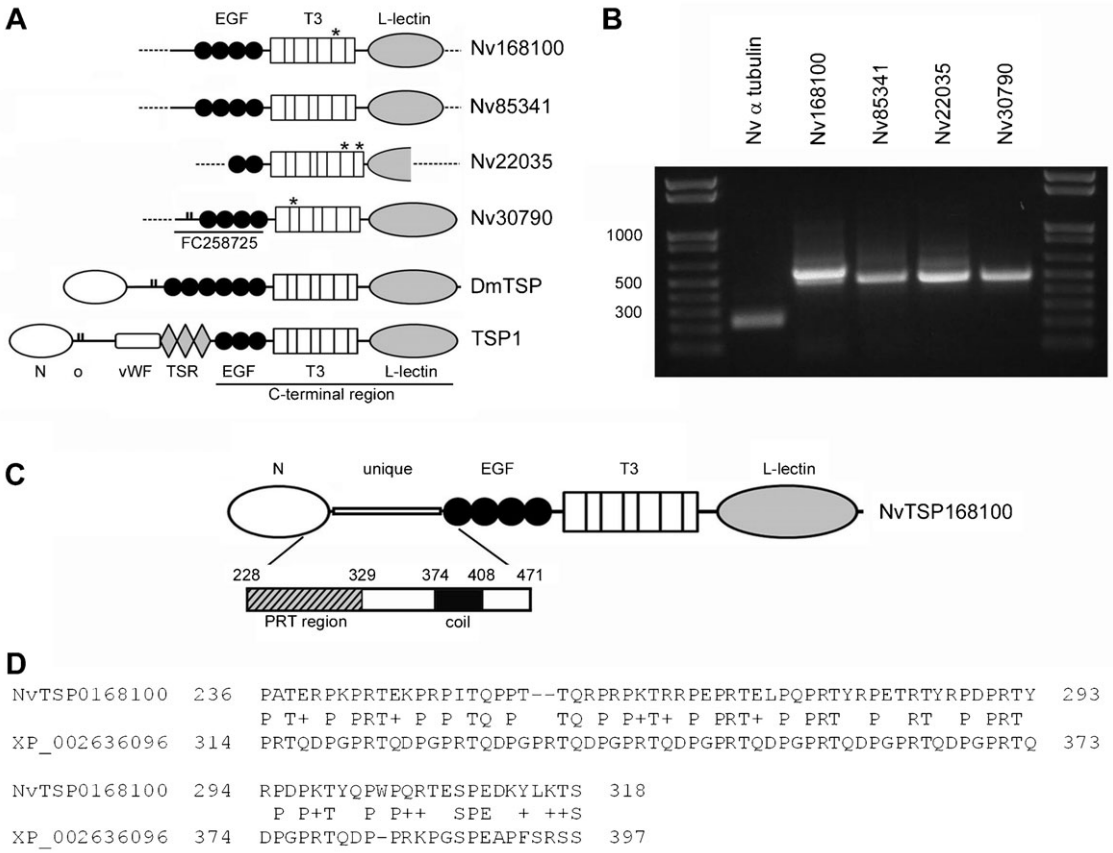

Fig. 1. The thrombospondins of *Nematostella vectensis*. (**A**) Schematic diagrams of protein domain organizations according to the *N. vectensis* genome assembly v1.0 transcript predictions at the Joint Genome Institute. The Nv30790 prediction is extended at the N-terminal end by the sequence of EST FC258725. Dashed lines indicate where predictions are incomplete in terms of thrombospondin domain organization. Representative pentameric (*D. melanogaster* TSP; DmTSP) and trimeric (vertebrate TSP-1; TSP1) thrombospondins are shown below. Asterisks indicate RGD and KGD motifs in the *N. vectensis* thrombospondins, and vertical lines indicate paired cysteine residues. EGF, epidermal growth factor-like domain; N, N-terminal domain; o, oligomerization domain; T3, thrombospondin type 3 repeat; vWF, von Willebrand factor type C domain. (**B**) RT-PCR confirms the presence of transcripts corresponding to each of the predicted *N. vectensis* thrombospondins in the adult. (**C**) Predicted protein domain organization from the complete cDNA of NvTSP168100. The polypeptide includes a unique region between the N-terminal domain and the EGF-like domains domain, and a C-terminal region with domain organization typical of subgroup B thrombospondins. PRT, region rich in proline, arginine and threonine. (**D**) Sequence homology between the PRT region of NvTSP168100 and a predicted protein of unknown function from *Caenorhabditis briggsae*, as identified from BLASTP searches.

corresponds to a canonical thrombospondin C-terminal region (Fig. 1A,C).

Phylogenetic analyses

Thrombospondins are widespread throughout the metazoa and *N. vectensis* is unusual as an early-diverging metazoan that encodes multiple thrombospondins (Bentley and Adams, 2010). Phylogenetic analyses were carried out to examine the relationships of *N. vectensis* thrombospondins to previously identified thrombospondins. Sequences corresponding to the conserved C-terminal regions (comprising three EGF-like domains, the type 3 repeats and the L-lectin domain) (Fig. 1A) were aligned by the MUSCLE algorithm and analyzed for phylogenetic relationships by neighborhood-joining or maximum-likelihood methods. Nv22035 was excluded from this analysis because the sequence prediction does not include the complete C-terminal region (Fig. 1A). The tree based on neighborhood-joining analysis was rooted between the TSP-DD group, which in these analyses also included the thrombospondin from the placozoan *Trichoplax adhaerens* and Nv85341, and all other thrombospondins (Fig. 3A). This tree demonstrated a close relationship between Nv116800 and Nv30790, consistent with the proposed origin from a lineage-specific gene duplication. The tree also indicated high diversity of the *N. vectensis* thrombospondins in that Nv116800 and Nv30790 appeared remote from Nv85341 and other thrombospondins (Fig. 3A). Maximum-likelihood analysis with boot-strapping extended these indications. The unrooted tree (Fig. 3B) confirmed the separate and robust groupings of A and DD group thrombospondins and the grouping of *T. adhaerens* thrombospondin and Nv85341 with the DD group. In this analysis, Nv116800 and Nv30790 clustered with the subgroup B thrombospondins of bilaterian protostomes and deuterostomes to form a large B group, albeit the rooting of this grouping was not well-supported by boot-strapping. Both methods indicated consistently that the C-terminal region of the thrombospondin from the demosponge *Amphimedon queenslandica* is remote from other thrombospondins; the maximum-likelihood analysis placed AqTSP on a separate branch from all other groups (Fig. 3B). To include Nv22035 in the analyses, an unrooted tree was also prepared based on only

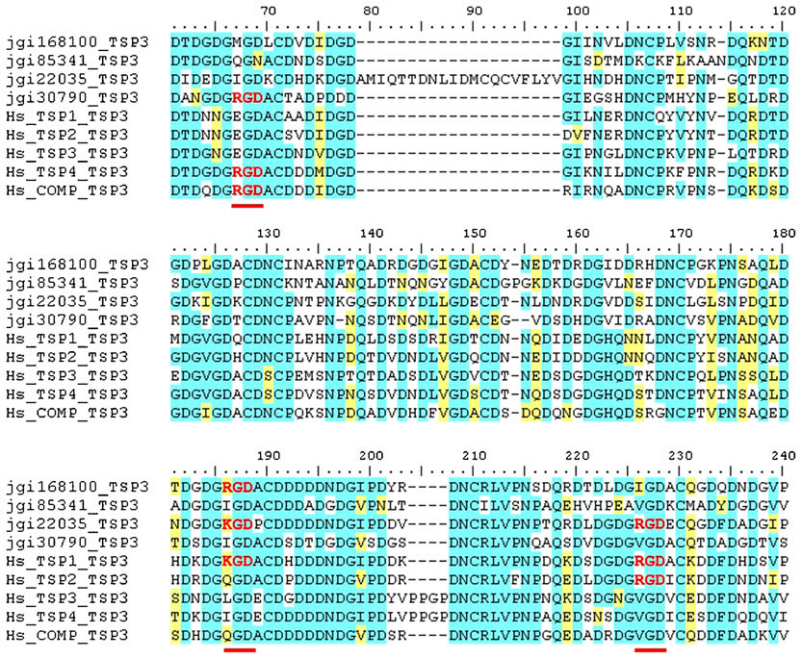

Fig. 2. RGD and KGD motifs in *N. vectensis* thrombospondins. The thrombospondin type 3 domains of the four *N. vectensis* thrombospondins and the five human thrombospondins were aligned with ClustalW (BioEdit). Identical residues are indicated in blue, and similar residues are indicated in yellow (BioEdit, default parameters). RGD or KGD residues that are found in one or more of the human thrombospondins are indicated in red and highlighted with a red line; one or more of the *N. vectensis* thrombospondins have an RGD or KGD motif (red) at the same location.

the type 3 repeats and L-lectin domain. This analysis placed Nv22035 separately from the previously described groups, not unlike the thrombospondin from *A. queenslandica*, and also placed the Nv116800/Nv30790 branch as a separate lineage related to both the A and B groups of TSPs (Fig. 3C).

The expression of a *Nematostella vectensis* thrombospondin

To localize NvTSP168100 in intact adult animals, a polyclonal antibody was raised in chickens against a portion of the N-terminal domain. The antibody was first characterized by immunoblotting. The polyclonal IgY recognized the antigen NvTSPN (Fig. 4A); this band was not seen following preabsorption of the antibody with antigen, nor was it present when the blot was incubated in preimmune IgY (not shown). The predicted molecular mass of NvTSP168100 is 130 kDa, and on immunoblots of the first pellet fraction (P1) of homogenized adult *N. vectensis* anti-NvTSP168100N recognized two bands running between 130 kDa and 250 kDa (arrowheads, Fig. 4A) and a third band running between 72 kDa and 95 kDa (arrow, Fig. 4A). These bands were not detected either with the preimmune IgY or after preabsorption of the antibody with antigen (not shown). The larger bands likely represent full length NvTSP168100 and are running higher than predicted due to posttranslational modifications such as glycosylation; the smaller band may result from proteolytic processing or may be a degradation product.

Immunohistochemistry was used to determine the sites of NvTSP168100 expression. Cross sections through the body column (scapus) of adult *N. vectensis* were incubated with anti-NvTSP168100N or with preimmune IgY and counterstained with TRITC-phalloidin (to show regions where myonemes, the cellular processes filled with retractile elements resembling striated muscle, are concentrated) and the nuclear stain DAPI. Immunostaining was seen in the mesoglea of retractor muscles in each of the mesenteries (i.e. the double folds of gastrodermis that project into the gastrovascular cavity) (Fig. 4B); the nearby parietal muscles were unlabeled as was the mesoglea found in adjacent sections incubated with preimmune serum (Fig. 4C). Adjacent sections incubated with preabsorbed anti-NvTSP168100N were also unlabeled (Fig. 4D). In longitudinal sections through the scapus of adult *N. vectensis* the nature of the immunolabeling of retractor muscles was clearer: the antibody labels long, beaded filaments or cell processes found between the longitudinally arrayed leaflets of the retractor muscle myonemes (Fig. 4E). In an oblique section through the mesoglea underlying the pharynx the anti-nTSP168100N labeled cell bodies with DAPI-stained nuclei and long narrow processes embedded within the mesoglea. The morphology of these cells and their processes was examined further by confocal and transmission electron microscopy. Confocal observations (Fig. 4G) revealed neuron-like triangular cell bodies labeled with anti-NvTSP168100N that are embedded within the mesoglea. Long, narrow, beaded processes with occasional branches extend from the cell bodies. Thin sections through the mesoglea of adult polyps revealed numerous cellular processes running longitudinally within the mesoglea of the retractor muscles (Fig. 4H). These processes have a relatively uniform cross sectional diameter of 300–350 nm. As observed in the confocal microscope, the processes were often found in loose bundles, though sometimes they were found singly. Higher magnification showed that these processes are closely associated with ECM within the mesoglea (Fig. 4H, inset). Most of the processes contain large membrane-bound vesicles and numerous small (30–40 nm) dark granules. In some of the processes microtubules were seen in cross section closely associated with the large vesicles. Similar processes were not observed in the mesoglea of the parietal muscles or the body wall (Tucker et al., 2011). Thus the cells that were immunostained with anti-NvTSP168100N bear a strong morphological resemblance to neurons and have processes that contain elements characteristic of neurites. These neuron-like cells are limited to the mesoglea of the pharynx and retractor muscles, where they are closely associated with the myonemes.

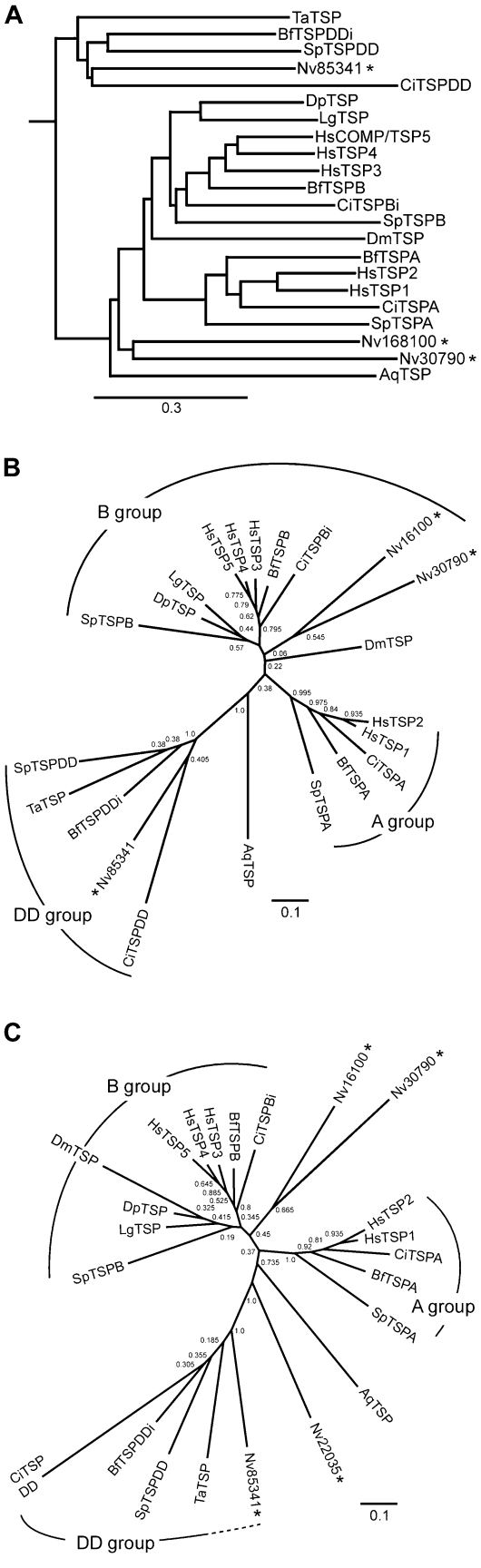

The expression of a *Nematostella vectensis* thrombospondin is upregulated during regeneration

We have shown previously that the ultrastructural appearance of the mesoglea in *N. vectensis* changes dramatically 48 hours after transection of the polyp (Tucker et al., 2011). To determine if the expression of NvTSP168100 changes during regeneration, 6-week-old polyps were transected and then processed for whole mount *in situ* hybridization 48 hours later. A signal was observed in the entire scapus, but the signal was strongest near the site of regeneration (Fig. 5A,B). To confirm upregulation of NvTSP168100 transcripts during regeneration we conducted quantitative PCR (qPCR) with NvTSP168100-specific primers and compared the level of expression in control polyps with the level of expression 48 hours after transection. qPCR confirmed the results of the *in situ* hybridization experiments, revealing a 41.8±11.1 (n=3) fold increase in the levels of NvTSP168100 mRNA following transection (Fig. 5C) (results were normalized to levels of a control rRNA). Next, immunohistochemistry was conducted on longitudinal sections through the scapus of polyps 48 hours following transection in order to confirm the results above and to localize the thrombospondin. The immunostaining of the neuron-like elements described above that are found within the mesoglea of the retractor muscles was still observed, but additional immunostaining was seen in the carbohydrate-rich lining of the epidermis known as the glycocalyx (Fig. 5D). This staining extended proximally toward the oral end of the column, where it abruptly ended (Fig. 5E). To determine if ultrastructural changes to the glycocalyx accompany regeneration, thin sections of the glycocalyx (preserved by using a fixative mixed with tannic acid and ruthenium red) were observed in the transmission electron microscope. In controls, the glycocalyx appeared as an electron-dense, fuzzy coat ~40–50 nm thick that lined the outer surface of the epidermis as well as the 1.5 µm long microvilli that protrude from the epidermis (Fig. 6A,B). This region was dramatically different 48 hours following transection: the microvilli were approximately twice as dense (3.2 microvilli/µm *versus* 1.4 microvilli/µm) and were often branched. Thin fibrils projected from the surface of the microvilli and often spanned the area between adjacent microvilli (Fig. 6C,D). Electron-dense debris appeared to be trapped at the outer limit of the microvilli and glycocalyx (Fig. 6B, arrows) and spherical elements ranging from 30–40 nm in diameter, which resembled viral particles, were associated with microvilli (Fig. 6D, arrowheads).

Fig. 3. Phylogenetic relationships of *N. vectensis* thrombospondins and other representative thrombospondins. In **A** and **B**, sequences of 620 residues including the last three EGF-like domains, thrombospondin type-3 repeats and the L-lectin-like domain from representative invertebrate and human thrombospondins were aligned in MUSCLE 3.7. (A) Rooted tree prepared by the neighborhood joining method in Phylip with proportionate branch lengths. (B) Unrooted tree prepared by the maximum-likelihood method in PHYML 3.0 with 200 cycles of bootstrapping. Bootstrap values are shown for each node; values above 0.7 are taken to indicate stability of the branchpoint. Scale bars show substitutions/site. *N. vectensis* thrombospondins are indicated by asterisks. (**C**) Unrooted tree prepared as in B, using only the sequences corresponding to the type 3 repeats and the L-lectin domain so as to include Nv22035. Aq, *Amphimedon queenslandica*; Bf, *Branchiostoma floridae*; Ci, *Ciona intestinalis*; Dp, *Daphnia pulex*; Dm, *Drosophila melanogaster*; Hs, *Homo sapiens*; Lg, *Lottia gigantea*; Nv, *Nematostella vectensis*; Sp, *Strongylocentrotus purpuratus*; Ta, *Trichoplax adhaerens*.

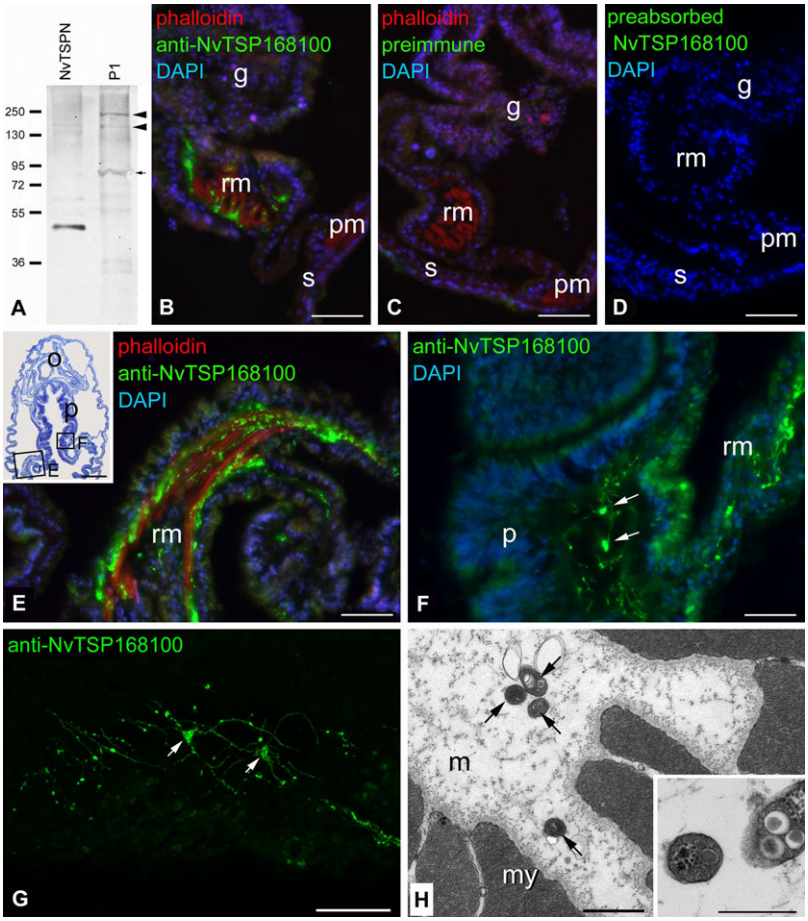

Fig. 4. Immunohistochemical analysis of the expression of *N. vectensis* thrombospondin 168100. (**A**) The chicken polyclonal anti-NvTSP168100 recognizes the antigen (NvTSPN) as well as two high molecular weight bands (arrowheads) and a smaller band (arrow) in the first pellet (P1) of an adult *N.vectensis* homogenate. Molecular weight markers are in kDa. (**B–D**) Cross sections through the column of an adult *N. vectensis* were incubated with anti-NvTSP168100 (B), preimmune antibody (C) or anti-NvTSP168100 preabsorbed with antigen (D). Anti-NvTSP168100 labels the mesoglea of the retractor muscles (rm) but not the parietal muscles (pm), body wall (s) or gonad (g). Scale bars=50 µm. (**E**) In longitudinal sections anti-NvTSP168100 labels beaded processes between the leaflets of the retractor muscle, which are stained with TRITC-phalloidin. Inset shows a neighboring section stained with toluidine blue, with the regions shown in E and F indicated with boxes. o, oral region; p, pharynx. Scale bar=50 µm (inset scale bar=250 µm). (**F**) Higher magnification of the region where a retractor muscle attaches to the thick-walled pharynx. Anti-NvTSP168100 stains thin processes and two cells (arrows) embedded within the mesoglea. Scale bar=25 µm. (**G**) Confocal imaging of the cells shown in F reveal triangular cell bodies (arrows) and neurite-like processes. Scale bar=25 µm. (**H**) The mesoglea of the retractor muscles contains numerous thin cell processes ~300 nm in diameter in cross section. Some are found in loose groups, while others are found singly (arrows). Scale bar=1 µm. The inset shows one of these processes at higher magnification. Inset scale bar=500 nm. m, mesoglea; my, myoneme.

Discussion

Based on the fossil record and molecular data, the divergence of Cnidaria and the Bilateria is estimated to have occurred around 750 million years ago, with Cnidaria subsequently evolving as a single phylum and the bilaterian ancestor giving rise to over 30 phyla (Ryan et al., 2007). In view of the diversity of bilaterians, the genome sequence of *N. vectensis* has proved very informative in illuminating the genomic complexity of the Eumetazoan ancestor. In relation to the protostomes examined to date, the gene content of *N. vectensis* includes large sets within gene families such as the Hox genes (Ryan et al., 2007). The encoding of four thrombospondins in *N. vectensis* also stands in contrast to the protostomes that have been examined to date and the demosponge *A. queenslandica*, all of which encode a single thrombospondin (Bentley and Adams, 2010; Srivastava et al., 2010). *N. vectensis* also encodes unexpectedly large families of SPARC-like proteins (Koehler et al., 2009) and integrins (Knack et al., 2008), indicating a propensity for retention of lineage-specific duplicated genes.

Analysis of the sequence relationships of the *N. vectensis* thrombospondins made on the basis of their conserved C-terminal regions demonstrated a high level of sequence diversity. Based on analysis of the entire C-terminal region, Nv168100 and Nv30790 were most related to the B group that also includes thrombospondins from protostomes and deuterostomes (Fig. 3B). All members of the B group examined experimentally to date have been found to assemble as pentamers. However, on the basis of its short coiled coil and unique PRT sequence region it is unlikely that Nv168100 assembles as a pentamer. Indeed, phylogenetic analysis of a shorter sequence region that permitted inclusion of all *N. vectensis* thrombospondins within the dataset, indicated that Nv168100 and Nv30790 may have diverged as a separate lineage from the inferred metazoan ancestor (Fig. 3C). Nv85341, along with *T. adhaerens* thrombospondin, was most related to the DD group, previously identified only in early-diverging deuterostomes (Bentley and Adams, 2010). Whether either Nv85341 or *T. adhaerens* thrombospondin contain an N-terminal discoidin domain must wait further sequencing studies, but it is interesting to consider the model that the DD group C-terminal region might have originated in the Eumetazoan ancestor, with subsequent loss from most protostome lineages. In line with other analyses of *A. queenslandica* gene content (Srivastava et al., 2010), the C-terminal region of *A. queenslandica* thrombospondin was distinct from all other thrombospondin sequences in the dataset. In the phylogenetic analysis of the shorter sequence region, including only the type 3 repeats and L-lectin domain, Nv22035 did not associate with any of the major thrombospondin groups and likely represents a lineage-specific divergence. This analysis, based on less sequence information, also moved Nv85341 to the edge of the DD group, but the central conclusion of great diversity of thrombospondin sequences within *N. vectensis* is upheld. Future analyses that include information from the yet-to-be sequenced genomes of other classes of cnidarians (e.g. the scyphozoa and cubozoa), as well as more complete *N. vectensis* sequences, may clarify these relationships.

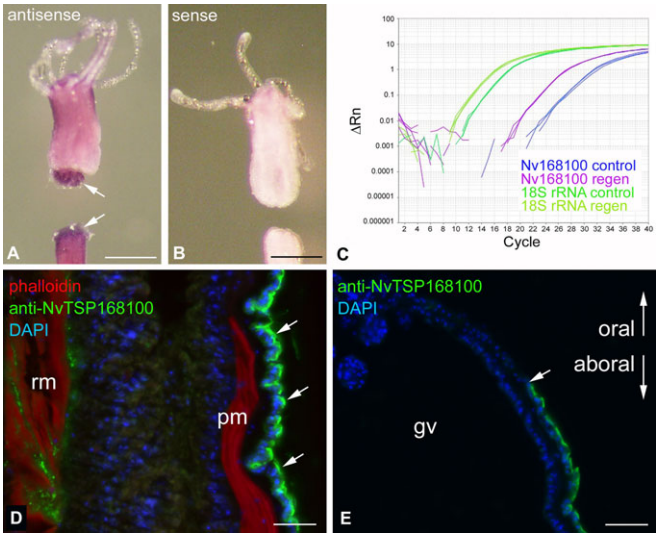

Fig. 5. Upregulation of *N. vectensis* thrombospondin 168100 during regeneration. (**A**,**B**) Juvenile polyps were fixed 48 hours following transection and processed for whole mount *in situ* hybridization with an antisense (A) or sense (B) probe to Nv168100. There is a superficial signal in the column wall of the polyp that appears stronger near the site of transection (arrows). Scale bars=500 µm. (**C**) Quantitative PCR reveals a 41.8±11.1 (n=3) fold increase in Nv168100 transcripts at 48 hours after transection. The fold increase was normalized to the levels of expression of an rRNA control transcript. (**D**,**E**) Longitudinal sections through the body wall of an adult *N. vectensis* polyp at 48 hours after transection were immunostained with anti-NvTSP168100. The antibody labels the glycocalyx lining the epidermis (arrows) in addition to the neuron-like elements in the retractor muscles (rm). The immunostaining of the glycocalyx ends near the oral end of the column (E). gv, gastrovascular cavity; pm, parietal muscle. Scale bars=25 µm (D,E).

With regard to potential ligands, most *N. vectensis* thrombospondins are candidate integrin ligands as three of the four thrombospondins contain one or more RGD or KGD motifs in their thrombospondin type 3 repeats that align with equivalent motifs of mammalian thrombospondins. *N. vectensis* encodes up to four beta integrins and three alpha integrins that represent

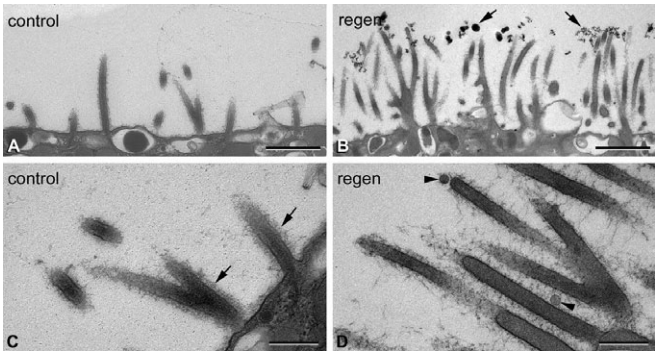

Fig. 6. Ultrastructural changes in the glycocalyx of *N. vectensis* during regeneration. The epidermal microvilli and glycocalyx of untransected (**A**,**C**) and regenerating (**B**,**D**) polyps is shown at low (A,B) and high (C,D) magnification. In the control polyps the microvilli are coated with a dense glycocalyx about 40–50 nm in thickness. Forty-eight hours after transection the microvilli are more abundant; a network of fine filaments spans the space between the microvilli. Spherical elements that resemble virus particles (arrowheads) are found near the microvilli and electron-dense material collects at the edge of the microvilli (arrows). Scale bars=1 µm (A,B) and 200 nm (C,D).

lineage-specific forms distinct from the functional groups recognized to be conserved in Bilateria (Knack et al., 2008). Thus, it cannot be predicted which of these integrins might bind to *N. vectensis* thrombospondins. NvTSP168100 has a canonical laminin G domain-like N-terminal domain containing motifs rich in basic residues and can be predicted to bind heparan glycosaminoglycans.

Complete predicted polypeptide sequence was obtained for NvTSP168100. The general domain organization has some unique features that make it unlike group B thrombospondins in other taxa. Most notable is the PRT region found between the N-terminal domain and the predicted coiled coil. This sequence aligns well with sequences from predicted proteins of unknown function in the nematode *C. briggsae* (Fig. 1D), and to a lesser extent with cell-wall proteins from some prokaryotes, but these similarities do not shed light on its potential function at this time. However, proline–arginine rich peptides derived from a small leucine-rich proteoglycan family member (PRELP) have been identified to have antimicrobial properties (e.g. Malmsten et al., 2006), which is intriguing given that NvTSP168100 appears to be upregulated in the glycocalyx after wounding and during regeneration. NvTSP168100 contains only a short coiled coil and is also lacking the characteristic cysteine residues that form interchain disulfide bonds adjacent to the oligomerization region in the pentameric group B thrombospondins. In the future, the oligomerization state of NvTSP168100 would need to be identified by biochemical analysis. Nv30790, the predicted thrombospondin that is closely related to NvTSP168100 in its C-terminal region (Fig. 2), does contain the characteristically spaced cysteine residues that are predicted to form interchain disulfide bonds, thus this feature of subunit assembly is highly conserved, albeit not in all *N. vectensis* thrombospondins. The domain organization of NvTSP168100 suggests that the encoding gene underwent domain shuffling resulting in the inclusion of the PRT region after a lineage-specific gene duplication event that gave rise to Nv30790 and NvTSP168100.

An antibody raised against the N-terminal sequences of NvTSP168100 labeled neuron-like cells embedded in the mesoglea of retractor muscles and the pharynx in adult *N. vectensis*. Morphologically these cells have the hallmark features of neurons, especially their long, beaded processes (which are indistinguishable at the level of the light microscope from the neuronal processes of *Hydra* (Grimmelikhuijzen and Westfall, 1995)) and the presence of dense-cored vesicles and longitudinally arrayed microtubules within these processes. The labeled cells could not be identified conclusively as neurons by double labeling with neuron-specific probes, as such probes have not yet been characterized in adult *N. vectensis*. Further studies in the adult with antibodies to neurotransmitters such as RFamide that identify subsets of neurons in planula larvae and juvenile polyps (Marlow et al., 2009) are called for. Neuronal immunostaining for a thrombospondin is not entirely unexpected, as others have shown that anti-thrombospondins readily label neurons in the central nervous system of mammals (e.g. Arber and Caroni, 1995). What is surprising is the presence of a population of neuron-like cells within the mesoglea, as ultrastructural analysis of adult anthozoans typically describes neuronal perikarya within the epidermis or gastrodermis (reviewed by Grimmelikhuijzen and Westfall, 1995). The mesoglea of *N. vectensis* is distinct from that of many other Cnidaria in containing cells, but to date the major cell type

recognized within the mesoglea is the amoebocyte, a migratory cell of the innate immune system (Frank and Bleakney, 1976; Tucker et al., 2011). Experiments with a promoter reporter transgene have suggested that the retractor and tentacles muscles have different gene expression profiles to other myoepithelial cells; these might include cues that promote nerve–muscle interactions in this body region where fast, dynamic movements are very important for prey engulfment (Renfer et al., 2010).

Very little is known about the molecular events that mediate regeneration in anthozoans. It is recognized that the process differs from wound repair (e.g. wounds that do not transect the body column do not lead to regeneration) and has features in common with events of embryogenesis. In *N. vectensis*, as in other Cnidaria, canonical Wnt signaling appears to have an important role in controlling regeneration (Trevino et al., 2011). ECM would be expected to have a role in regeneration and, indeed, in transected adult *N. vectensis*, morphological reorganization of the mesoglea is apparent in the region adjacent to the transection site (Tucker et al., 2011). Here, we demonstrate that the epidermal glycocalyx is also reorganized during regeneration and that NvTSP168100 is a likely participant in this reorganization, as demonstrated by its upregulation and prominent altered localization. Further studies of the cellular and biochemical properties of NvTSP168100, as well as further knowledge of the other *N. vectensis* thrombospondins, will provide additional insights into the evolution of tissues and homeostatic cell–ECM interactions.

Materials and Methods

Nematostella culture

A colony of mature *N. vectensis* polyps descended from clones CH2 and CH6 (Hand and Uhlinger, 1992) were obtained from the University of California Davis Bodega Bay Marine Laboratory. The sea anemones were maintained in microfiltered sea water diluted to 33% with distilled water at room temperature and adjusted to pH 7.8. Details of raising the sea anemones can be found in Darling et al. and Tucker (Darling et al., 2005; Tucker, 2010), and details associated with transecting the polyps to study regeneration can be found in Tucker et al. (Tucker et al., 2011).

Gene identification, expression analysis and molecular cloning

Putative thrombospondin genes were identified in the genome of *N. vectensis* (Putnam et al., 2007) by BLAST (http://blast.ncbi.nlm.nih.gov) searches of JGI transcripts and by using the Superfamily database (http://supfam.cs.bris.ac.uk/SUPERFAMILY) searching for predicted proteins with multiple domains characteristic of thrombospondins that were present in the right order. Further domain analysis of the predicted proteins was carried out using Pfam (http://pfam.sanger.ac.uk) and SMART (http://smart.embl-heidelberg.de).

The expression of the putative thrombospondins in adult *N. vectensis* polyps was confirmed using reverse transcriptase polymerase chain reaction (RT-PCR). Methods for polyA mRNA isolation and PCR amplification conditions were described previously (Tucker, 2010). The primers used to amplify products corresponding to the putative thrombospondin sequences identified above were: 5′-GATACCGCCCTAACACAGGA-3′ and 5′-CGTGTCTAGTTGTGCGCTGT-3′ (Nv168100, XP_1631622; 500 bp product; these primers were also used as described below and called NvTSP168100F/R); 5′-CCTGGTTTTATCGGACATGG-3′ and 5′-TACCATCACCGTCGCTATCA-3′ (Nv85341, XP_1639928; 499 bp product); 5′-GACCTTGATGGATTCCCAGA-3′ and 5′-CCGTCATGATCACTGTCCAC-3′ (Nv22035; 503 bp product); and 5′-TCATGACAACTGCCCTACCA-3′ and 5′-TCTGGCCATTTACGCCTATC-3′ (Nv30790; 501 bp product). Each of the primer pairs above spanned introns to control for DNA contamination. In addition, a control primer pair corresponding to α-tubulin sequences was used (Tucker, 2010). Primers were ordered from Eurofins MWG Operon and size standards were purchased from Invitrogen. The PCR products were subcloned using a TOPO TA-Cloning kit (Invitrogen) into pCRII or pCR2.1 cloning vectors and sequenced by Davis Sequencing.

One of the putative thrombospondins (Nv168100, XP_1631622) was cloned to generate a potentially complete cDNA sequence using primers based on the predicted transcript as well as potential open reading frame sequences identified from the genome both 3′ and 5′ to the JGI predicted transcript to create five overlapping PCR products: NvTSP168100N2, NvTSP168100N, NvTSP168100 (the PCR product described above), NvTSP16800C and NvTSP168100C2. This expanded the predicted protein to include a thrombospondin-type N-terminal domain with a potential in-frame start codon and signal peptide and a complete L-lectin domain with an in-frame stop codon. The primer pairs used to generate the overlapping PCR products were: NvTSP168100N2F (5′-CTTGCTATGGGCTGCCTGT-3′), NvTSP168100NR (5′-CGACATGCTCCTCCTTTCTC-3′), nTSP168100NF (5′-AGTCCAACGCGTTCCATTAC-3′), NvTSP168100NR (5′-CATCGGCGTCATATTCACAG-3′), NvTSP168100F (5′- GATACCGCCCTAACACAGGA-3′), NvTSP168100R (5′-CGTGTCTAGTTGTGCGCTGT-3′), NvTSP16800CF (5′-TGATAACTGCCCAGGGAAAC-3′), NvTSP16800CR (5′-TCCACTGTGCCATAGAGCAT-3′), NvTSP168100C2F (5′-TGGGTACCAGGATTACAGC-3′) and NvTSP168100C2R (5′-TTGCATGACATGGGTTGTGT-3′). The PCR products were subcloned and sequenced as described above. The complete cDNA sequence is deposited as GenBank accession number JX680803.

Bioinformatics and phylogenetic analyses

Domain architectures of the predicted *N. vectensis* thrombospondin polypeptides were analyzed against the InterproScan database (Quevillon et al., 2005) at EBI (http://www.ebi.ac.uk/Tools/pfa/iprscan). Coiled-coil domains were identified with the COILs algorithm, with 2.5 fold weighting applied for the a and d positions (Lupas et al., 1991). Domain boundaries were assigned by MUSCLE (Edgar, 2004) multiple sequence alignment of the *N. vectensis* thrombospondins against well-characterized thrombospondins. Phylogenetic analyses were based on a previously developed dataset of thrombospondin sequences (Bentley and Adams, 2010). This dataset was curated for the current study by inclusion of *Amphimendon queenslandica* thrombospondin (GenBank XP_003389217) (Srivastava et al., 2010) and limitation of vertebrate thrombospondin sequences to human TSP1–5. Multiple sequence alignment of sequences of ~620 residues, corresponding to the last three EGF domains to C-terminus of these proteins (or, to include Nv22035 in the analysis, only the residues corresponding to the type 3 repeats and the L-lectin domain), was made in MUSCLE 3.7. For tree construction, variations present in <5% of the sequences leading to gapping were removed from the alignment. Trees were constructed by neighborhood-joining in Phylip v3.6 (Felsenstein, J., distributed by the author; Department of Genome Sciences, University of Washington, Seattle, 2004) and maximum likelihood in PhyML 3.0 (Guindon et al., 2010) at default parameters with 200 cycles of boot-strapping. Analyses were carried out through the resources of Phylogeny.fr (http://www.phylogeny.fr) (Dereeper et al., 2008), and Phylemon 2.0 (http://phylemon.bioinfo.cipf.es) (Sánchez et al., 2011).

Protein expression and antibody production

Plasmid NvTSP168100N2 (pTSPN) was the source for DNA sequences used to express a recombinant partial N-terminal thrombospondin domain of NvTSP168100 for antibody production. pTSPN was digested with *Eco*RI to release an ~1.1 kb fragment encoding aa 67 to aa 437 of the presumptive protein. This fragment was cloned into pT7(-1) (pT7-7) (Studier et al., 1990) with a one nucleotide deletion to change the reading frame. The resulting plasmid was sequenced to verify DNA sequence and orientation then introduced into BL21-AI (Invitrogen) for large scale expression. Protein expression was induced by the addition of 0.5 g of arabinose to 500 ml of exponentially growing *E. coli* at an OD600 ~0.8. After 5–6 hours of induction cells were harvested by centrifugation and stored as wet pellets at −20℃ until processed. The recombinant protein readily formed inclusion bodies that were purified using lysozyme/detergent lysis with DNase/RNase digestion followed by high salt and low salt washes (Nagai and Thøgersen, 1987). Purified inclusion bodies were resuspended in 10 mM Tris pH 7.5, 1 mM EDTA, 0.2 M NaCl, 8 M urea and chromatographed on a GE Healthcare HiLoad 16/60 Superdex 200 gel filtration column. Fractions were monitored by SDS-PAGE and peak fractions pooled. Protein concentration was determined using a Pierce BCA assay with BSA as a standard (Thermo Scientific). Recombinant protein was dialyzed against PBS overnight to remove urea; the majority of the protein precipitated.

Preimmune chicken antibodies (made from 3 eggs prior to injection) and purified chicken anti-NvTSP168100N IgY were prepared at Aves Labs.

Paraffin embedding and immunohistochemistry

Adult *N. vectensis* polyps were immersed in 7.5% $MgCl_2$ in 33% sea water for 20 minutes, fixed in 2% paraformaldehyde in phosphate buffered saline (PBS) at room temperature for 30 minutes, then fixed for 5 hours in 4% paraformaldehyde in PBS at 4℃. After rinsing overnight in cold PBS the specimens were trimmed using a razor blade and dehydrated in increasing concentrations of ethanol (50%, 75%, 95%; 10 minutes/solution) to 100% ethanol (two changes, 10 minutes each). The specimens were then cleared in xylene (two changes, 5 minutes each), infiltrated with two changes of paraffin (63℃, 1 hour each) and embedded in paraffin blocks. Sections were cut at 8 µm and collected after floating in a warm water bath onto presubbed slides (Superfrost Plus, Fisher Scientific). Sections were deparaffinized and rehydrated (two changes of xylene, 100% and 95% ethanol,

5 minutes each, followed by 5 minutes in 75% ethanol, two changes of water and two changes of PBS) and either stained with toluidine blue or processed for immunohistochemistry. For immunohistochemistry, sections were blocked in 0.5% BSA in PBS for 30 minutes, then incubated overnight at room temperature in diluted preimmune IgY, anti-NvTSP168100 IgY, or anti-NvTSP168100 IgY preabsorbed with antigen in BSA/PBS. Sections were then rinsed three times in PBS and incubated for 2 hours in diluted Cy2-tagged donkey anti-chicken secondary antibody (Molecular Probes) in a 1:50 solution of TRITC-phalloidin (Sigma). The sections were then rinsed twice in PBS, stained with a 1:10,000 solution of Hoechst 33258 (DAPI; Molecular Probes) in PBS for 1 minute, rinsed again in PBS, and mounted in 1:1 glycerol/PBS. Slides were observed and photographed using a Nikon Eclipse E800 photomicroscope and an Olympus IX81 confocal microscope.

In situ hybridization and quantitative PCR

Whole mount *in situ* hybridization was conducted using methods described previously (Tucker, 2010; based on methods found in Martindale et al., 2004). Antisense and sense NvTSP 168100 digoxygenin-labeled riboprobes were made using reagents supplied by Boehringer Mannheim; this was also the commercial source of the anti-digoxygenin and the colorization substrates.

For qPCR three animals per sample were pooled in a 1 ml homogenizer, lysed with 500 µl of Trizol and homogenized. The lysate was sheared through a 26 gauge needle until little to no resistance was felt though the syringe. Samples were then incubated on ice for 15 minutes followed by 5 minutes at room temperature. 100 µl of chloroform was added to each sample, which was then shaken vigorously for 15 seconds and allowed to separate at room temperature for 5 minutes. Samples were spun at 14 k for 15 minutes at 4℃ and the chloroform layer was removed and transferred to a new tube with 250 µl of ice-cold isopropanol. The sample was allowed to precipitate at room temperature for 10 minutes, then centrifuged at 14 k for 15 minutes at 4℃. The RNA pellet was rinsed with 1 ml of 70% ethanol and then spun at 14 k for 5 minutes. The resulting pellet was air dried and suspended in RNase-free water. The quality and quantity of RNA was determined by gel electrophoresis and a Nanodrop spectrophotometer. One µg of total RNA was reverse transcribed into cDNA by incubating for 1 hour at 37℃ using AMV Reverse Transcriptase (Affymetrix) and oligo dT primers. Three cDNA replicates of each treatment (control or regenerating) were used to conduct the qPCR. The composition of the PCR mix for each sample was as follows: 10 µl of 30× diluted sample, reverse primer (1 µM; 5′-GGTCCCGTAACCGACC-AGTGTCC-3′), forward primer (1 µM; 5′-CAAAGAGGCTGGAGACAT-CGAGTTGC-3′) and 12.5 µl of SybrGreen I Master Mix (Applied Biosystems). Control primers were based on 18S rRNA sequences (Reitzel and Tarrant, 2009) (5′-GACTCAACACGGGGAAACTC-3′ and 5′-GCACCACCACCCATAGAAT-C-3′). The amplification program was as follows: an initial denaturing step at 95℃ (10 minutes), followed by 40 cycles of 95℃ (30 seconds) and 60℃ (30 seconds). A melting curve was obtained from a first step starting from 50 to 95℃ to control for each primer pair. For each of the three replicates of a sample, the average cycle time (Ct) and the standard deviation (stdev) were calculated. For each sample, the average Ct of the Gene of Interest (GOI) (avg. Ct_{GOI}) was normalized to the average Ct of the reference gene (avg. Ct_{ref}) for the same sample to calculate the normalized Ct for the GOI (ΔCt=avg. Ct_{GOI}/avg. Ct_{ref}). The stdev of the ΔCt was calculated, and the $\Delta\Delta CT$, or calibrated value, for each sample was given by this formula: $\Delta Ct_R - \Delta Ct_U$. The stdev of $\Delta\Delta Ct$ was the same as the stdev of ΔCt. The fold-induction for each sample relative to the calibrator$=2^{(-\Delta\Delta Ct)}$.

Electron microscopy

Specimens were prepared for thin sectioning and electron microscopy as described previously (Tucker et al., 2011). In short, adult *N. vectensis* that had been transected 48 hours previously (n=2) or untransected animals (n=2) were immersed in 7.5% $MgCl_2$ in 33% sea water for 20 minutes, then fixed overnight in ice-cold 2.5% gluteraldehyde (Polysciences) in 100 mM sodium cacodylate (Sigma) buffer. To improve the retention and electron density of glycoproteins, the fixative also contained 0.1% tannic acid (Polysciences) and 0.1% ruthenium red (Sigma) (Luft, 1971). The regenerating specimens were trimmed so that the glycocalyx near the site of regeneration could be observed in longitudinal section. The specimens were then rinsed, postfixed in 1% OsO_4 with 0.1% ruthenium red, embedded, sectioned and stained using traditional methods. Stained thin sections were viewed and photographed using a Philips CM210 transmission electron microscope.

Acknowledgements

We are indebted to Thomas Blankenship for his assistance with the electron microscopy, to Mark Q. Martindale for sharing details of the whole mount *in situ* hybridization protocol and to Carol Vines for helping us establish a colony of *N. vectensis*. This research received no specific grant from any funding agency in the public, commercial or not-for-profit sectors.

Competing Interests

The authors have no competing interests to declare.

References

Adams, J. C. and Lawler, J. (2012). The thrombospondins. In *Extracellular Matrix Biology* (ed. R. O. Hynes and K. M. Yamada), pp. 99-127. Cold Spring Harbor, NY: Cold Spring Harbor Laboratory Press.

Adams, J. C., Monk, R., Taylor, A. L., Özbek, S., Fascetti, N., Baumgartner, S. and Engel, J. (2003). Characterisation of *Drosophila* thrombospondin defines an early origin of pentameric thrombospondins. *J. Mol. Biol.* **328**, 479-494.

Arber, S. and Caroni, P. (1995). Thrombospondin-4, an extracellular matrix protein expressed in the developing and adult nervous system promotes neurite outgrowth. *J. Cell Biol.* **131**, 1083-1094.

Bentley, A. A. and Adams, J. C. (2010). The evolution of thrombospondins and their ligand-binding activities. *Mol. Biol. Evol.* **27**, 2187-2197.

Chanana, B., Graf, R., Koledachkina, T., Pflanz, R. and Vorbrüggen, G. (2007). α_{PS2} integrin-mediated muscle attachment in *Drosophila* requires the ECM protein Thrombospondin. *Mech. Dev.* **124**, 463-475.

Chapman, J. A., Kirkness, E. F., Simakov, O., Hampson, S. E., Mitros, T., Weinmaier, T., Rattei, T., Balasubramanian, P. G., Borman, J., Busam, D. et al. (2010). The dynamic genome of *Hydra*. *Nature* **464**, 592-596.

Darling, J. A., Reitzel, A. R., Burton, P. M., Mazza, M. E., Ryan, J. F., Sullivan, J. C. and Finnerty, J. R. (2005). Rising starlet: the starlet sea anemone, *Nematostella vectensis*. *Bioessays* **27**, 211-221.

Dereeper, A., Guignon, V., Blanc, G., Audic, S., Buffet, S., Chevenet, F., Dufayard, J. F., Guindon, S., Lefort, V., Lescot, M. et al. (2008). Phylogeny.fr: robust phylogenetic analysis for the non-specialist. *Nucleic Acids Res.* **36 suppl. 2**, W465-W469.

Edgar, R. C. (2004). MUSCLE: a multiple sequence alignment method with reduced time and space complexity. *BMC Bioinformatics* **5**, 113.

Frank, P. and Bleakney, J. S. (1976). Histology and sexual reproduction of the anemone *Nematostella vectensis* Stephenson 1935. *J. Nat. Hist.* **10**, 441-449.

Gilsohn, E. and Volk, T. (2010). Slowdown promotes muscle integrity by modulating integrin-mediated adhesion at the myotendinous junction. *Development* **137**, 785-794.

Grimmelikhuijzen, C. J. P. and Westfall, J. A. (1995). The nervous system of Cnidarians. In *The Nervous Systems Of Invertebrates: Evolutionary And Comparative Approach* (ed. O. Breidbach and W. Kutsch). Basel: Birkhäuser Verlag.

Guindon, S., Dufayard, J. F., Lefort, V., Anisimova, M., Hordijk, W. and Gascuel, O. (2010). New algorithms and methods to estimate maximum-likelihood phylogenies: assessing the performance of PhyML 3.0. *Syst. Biol.* **59**, 307-321.

Hand, C. and Uhlinger, K. R. (1992). The culture, sexual and asexual reproduction, and growth of the sea anemone *Nematostella vectensis*. *Biol. Bull.* **182**, 169-176.

Kasprick, D. S., Kish, P. E., Junttila, T. L., Ward, L. A., Bohnsack, B. L. and Kahana, A. (2011). Microanatomy of adult zebrafish extraocular muscles. *PLoS ONE* **6**, e27095.

Knack, B. A., Iguchi, A., Shinzato, C., Hayward, D. C., Ball, E. E. and Miller, D. J. (2008). Unexpected diversity of cnidarian integrins: expression during coral gastrulation. *BMC Evol. Biol.* **8**, 136.

Koehler, A., Desser, S., Chang, B., MacDonald, J., Tepass, U. and Ringuette, M. (2009). Molecular evolution of SPARC: absence of the acidic module and expression in the endoderm of the starlet sea anemone, *Nematostella vectensis*. *Dev. Genes Evol.* **219**, 509-521.

Luft, J. H. (1971). Ruthenium red and violet. I. Chemistry, purification, methods of use for electron microscopy and mechanism of action. *Anat. Rec.* **171**, 347-368.

Lupas, A., Van Dyke, M. and Stock, J. (1991). Predicting coiled coils from protein sequences. *Science* **252**, 1162-1164.

Malmsten, M., Davoudi, M. and Schmidtchen, A. (2006). Bacterial killing by heparin-binding peptides from PRELP and thrombospondin. *Matrix Biol.* **25**, 294-300.

Marlow, H. Q., Srivastava, M., Matus, D. Q., Rokhsar, D. and Martindale, M. Q. (2009). Anatomy and development of the nervous system of *Nematostella vectensis*, an anthozoan cnidarian. *Dev. Neurobiol.* **69**, 235-254.

Martindale, M. Q., Pang, K. and Finnerty, J. R. (2004). Investigating the origins of triploblasty: 'mesodermal' gene expression in a diploblastic animal, the sea anemone *Nematostella vectensis* (phylum, Cnidaria; class, Anthozoa). *Development* **131**, 2463-2474.

McKenzie, P., Chadalavada, S. C., Bohrer, J. and Adams, J. C. (2006). Phylogenomic analysis of vertebrate thrombospondins reveals fish-specific paralogues, ancestral gene relationships and a tetrapod innovation. *BMC Evol. Biol.* **6**, 33.

Mosher, D. F. and Adams, J. C. (2012). Adhesion-modulating/matricellular ECM protein families: a structural, functional and evolutionary appraisal. *Matrix Biol.* **31**, 155-161.

Nagai, K. and Thøgersen, H. C. (1987). Synthesis and sequence-specific proteolysis of hybrid proteins produced in *Escherichia coli*. *Methods Enzymol.* **153**, 461-481.

Özbek, S., Balasubramanian, P. G., Chiquet-Ehrismann, R., Tucker, R. P. and Adams, J. C. (2010). The evolution of extracellular matrix. *Mol. Biol. Cell* **21**, 4300-4305.

Putnam, N. H., Srivastava, M., Hellsten, U., Dirks, B., Chapman, J., Salamov, A., Terry, A., Shapiro, H., Lindquist, E., Kapitonov, V. V. et al. (2007). Sea anemone genome reveals ancestral eumetazoan gene repertoire and genomic organization. *Science* **317**, 86-94.

Quevillon, E., Silventoinen, V., Pillai, S., Harte, N., Mulder, N., Apweiler, R. and Lopez, R. (2005). InterProScan: protein domains identifier. *Nucleic Acids Res.* **33 suppl. 2**, W116-W120.

Reitzel, A. M. and Tarrant, A. M. (2009). Nuclear receptor complement of the cnidarian *Nematostella vectensis*: phylogenetic relationships and developmental expression patterns. *BMC Evol. Biol.* **9**, 230.

Renfer, E., Amon-Hassenzahl, A., Steinmetz, P. R. and Technau, U. (2010). A muscle-specific transgenic reporter line of the sea anemone, *Nematostella vectensis*. *Proc. Natl. Acad. Sci. USA* **107**, 104-108.

Risher, W. C. and Eroglu, C. (2012). Thrombospondins as key regulators of synaptogenesis in the central nervous system. *Matrix Biol.* **31**, 170-177.

Ruoslahti, E. (1996). RGD and other recognition sequences for integrins. *Annu. Rev. Cell Dev. Biol.* **12**, 697-715.

Ryan, J. F., Mazza, M. E., Pang, K., Matus, D. Q., Baxevanis, A. D., Martindale, M. Q. and Finnerty, J. R. (2007). Pre-bilaterian origins of the Hox cluster and the Hox code: evidence from the sea anemone, *Nematostella vectensis*. *PLoS ONE* **2**, e153.

Sánchez, R., Serra, F., Tárraga, J., Medina, I., Carbonell, J., Pulido, L., de María, A., Capella-Gutíerrez, S., Huerta-Cepas, J., Gabaldón, T. et al. (2011). Phylemon 2.0: a suite of web-tools for molecular evolution, phylogenetics, phylogenomics and hypotheses testing. *Nucleic Acids Res.* **39 suppl. 2**, W470-W474.

Schmid, V., Ono, S. I. and Reber-Müller, S. (1999). Cell-substrate interactions in cnidaria. *Microsc. Res. Tech.* **44**, 254-268.

Srivastava, M., Simakov, O., Chapman, J., Fahey, B., Gauthier, M. E., Mitros, T., Richards, G. S., Conaco, C., Dacre, M., Hellsten, U. et al. (2010). The *Amphimedon queenslandica* genome and the evolution of animal complexity. *Nature* **466**, 720-726.

Studier, F. W., Rosenberg, A. H., Dunn, J. J. and Dubendorff, J. W. (1990). Use of T7 RNA polymerase to direct expression of cloned genes. *Methods Enzymol.* **185**, 60-89.

Subramanian, A., Wayburn, B., Bunch, T. and Volk, T. (2007). Thrombospondin-mediated adhesion is essential for the formation of the myotendinous junction in *Drosophila*. *Development* **134**, 1269-1278.

Tan, K., Duquette, M., Liu, J. H., Zhang, R., Joachimiak, A., Wang, J. H. and Lawler, J. (2006). The structures of the thrombospondin-1 N-terminal domain and its complex with a synthetic pentameric heparin. *Structure* **14**, 33-42.

Trevino, M., Stefanik, D. J., Rodriguez, R., Harmon, S. and Burton, P. M. (2011). Induction of canonical Wnt signaling by alsterpaullone is sufficient for oral tissue fate during regeneration and embryogenesis in *Nematostella vectensis*. *Dev. Dyn.* **240**, 2673-2679.

Tucker, R. P. (1993). The in situ localization of tenascin splice variants and thrombospondin 2 mRNA in the avian embryo. *Development* **117**, 347-358.

Tucker, R. P. (2010). Expression of usherin in the anthozoan *Nematostella vectensis*. *Biol. Bull.* **218**, 105-112.

Tucker, R. P., Adams, J. C. and Lawler, J. (1995). Thrombospondin-4 is expressed by early osteogenic tissues in the chick embryo. *Dev. Dyn.* **203**, 477-490.

Tucker, R. P., Shibata, B. and Blankenship, T. N. (2011). Ultrastructure of the mesoglea of the sea anemone *Nematostella vectensis* (Edwardsiidae). *Invertebr. Biol.* **130**, 11-24.

Urry, L. A., Whittaker, C. A., Duquette, M., Lawler, J. and DeSimone, D. W. (1998). Thrombospondins in early *Xenopus* embryos: dynamic patterns of expression suggest diverse roles in nervous system, notochord, and muscle development. *Dev. Dyn.* **211**, 390-407.